



Designation: E2860 – 20

Standard Test Method for Residual Stress Measurement by X-Ray Diffraction for Bearing Steels¹

This standard is issued under the fixed designation E2860; the number immediately following the designation indicates the year of original adoption or, in the case of revision, the year of last revision. A number in parentheses indicates the year of last reapproval. A superscript epsilon (ϵ) indicates an editorial change since the last revision or reapproval.

INTRODUCTION

The measurement of residual stress using X-ray diffraction (XRD) techniques has gained much popularity in the materials testing field over the past half century and has become a mandatory test for many production and prototype bearing components. However, measurement practices have evolved over this time period. With each evolutionary step, it was discovered that previous assumptions were sometimes erroneous, and as such, results obtained were less reliable than those obtained using state-of-the-art XRD techniques. Equipment and procedures used today often reflect different periods in this evolution; for example, systems that still use the single- and double-exposure techniques as well as others that use more advanced multiple exposure techniques can all currently be found in widespread use. Moreover, many assumptions made, such as negligible shear components and non-oscillatory $\sin^2\psi$ distributions, cannot safely be made for bearing materials in which the demand for measurement accuracy is high. The use of the most current techniques is, therefore, mandatory to achieve not only the most reliable measurement results but also to enable identification and evaluation of potential measurement errors, thus paving the way for future developments.

1. Scope*

1.1 This test method covers a procedure for experimentally determining macroscopic residual stress tensor components of quasi-isotropic bearing steel materials by X-ray diffraction (XRD).

1.2 This test method provides a guide for experimentally determining stress values, which play a significant role in bearing life.

1.3 Examples of how tensor values are used are:

- 1.3.1 Detection of grinding type and abusive grinding;
- 1.3.2 Determination of tool wear in turning operations;
- 1.3.3 Monitoring of carburizing and nitriding residual stress effects;
- 1.3.4 Monitoring effects of surface treatments such as sand blasting, shot peening, and honing;
- 1.3.5 Tracking of component life and rolling contact fatigue effects;
- 1.3.6 Failure analysis;
- 1.3.7 Relaxation of residual stress; and

¹ This test method is under the jurisdiction of ASTM Committee E28 on Mechanical Testing and is the direct responsibility of Subcommittee E28.13 on Residual Stress Measurement.

Current edition approved Nov. 1, 2020. Published February 2021. Originally approved in 2012. Last previous edition approved in 2012 as E2860–12. DOI: 10.1520/E2860–20.

1.3.8 Other residual-stress-related issues that potentially affect bearings.

1.4 *Units*—The values stated in SI units are to be regarded as standard. No other units of measurement are included in this standard.

1.5 *This standard does not purport to address all of the safety concerns, if any, associated with its use. It is the responsibility of the user of this standard to establish appropriate safety, health, and environmental practices and determine the applicability of regulatory limitations prior to use.*

1.6 *This international standard was developed in accordance with internationally recognized principles on standardization established in the Decision on Principles for the Development of International Standards, Guides and Recommendations issued by the World Trade Organization Technical Barriers to Trade (TBT) Committee.*

2. Referenced Documents

- 2.1 *ASTM Standards*:²
 - E6 Terminology Relating to Methods of Mechanical Testing
 - E7 Terminology Relating to Metallography

² For referenced ASTM standards, visit the ASTM website, www.astm.org, or contact ASTM Customer Service at service@astm.org. For *Annual Book of ASTM Standards* volume information, refer to the standard's Document Summary page on the ASTM website.

*A Summary of Changes section appears at the end of this standard

E177 Practice for Use of the Terms Precision and Bias in ASTM Test Methods

E691 Practice for Conducting an Interlaboratory Study to Determine the Precision of a Test Method

E915 Test Method for Verifying the Alignment of X-Ray Diffraction Instrumentation for Residual Stress Measurement

E1426 Test Method for Determining the X-Ray Elastic Constants for Use in the Measurement of Residual Stress Using X-Ray Diffraction Techniques

2.2 ANSI Standards.³

N43.2 Radiation Safety for X-ray Diffraction and Fluorescence Analysis Equipment

N43.3 For General Radiation Safety—Installations Using Non-Medical X-Ray and Sealed Gamma-Ray Sources, Energies Up to 10 MeV

2.3 SAE standard.⁴

HS-784/2003 Residual Stress Measurement by X-Ray Diffraction, 2003 Edition

3. Terminology

3.1 Definitions—Many of the terms used in this test method are defined in Terminologies E6 and E7.

3.2 Definitions of Terms Specific to This Standard:

3.2.1 interplanar spacing, n —perpendicular distance between adjacent parallel atomic planes.

3.2.2 macrostress, n —average stress acting over a region of the test specimen containing many grains/crystals/coherent domains.

3.3 Abbreviations:

3.3.1 ALARA—As low as reasonably achievable

3.3.2 FWHM—Full width half maximum

3.3.3 LPA—Lorentz-polarization-absorption

3.3.4 MSDS—Material safety data sheet

3.3.5 XEC—X-ray elastic constant

3.3.6 XRD—X-ray diffraction

3.4 Symbols: $\frac{1}{2} S_2^{(hkl)}$ = X-ray elastic constant of quasi-isotropic material equal to $\frac{1+\nu}{E^{(hkl)}}$

³ Available from American National Standards Institute (ANSI), 25 W. 43rd St., 4th Floor, New York, NY 10036, <http://www.ansi.org>.

⁴ Available from SAE International (SAE), 400 Commonwealth Dr., Warrendale, PA 15096, <http://www.sae.org>.

α_L = Linear thermal expansion coefficient
 β = Angle between the incident beam and σ_{33} or surface normal on the σ_{33} σ_{11} plane
 χ = Angle between the $\sigma_{\varphi+90^\circ}$ direction and the normal to the diffracting plane
 χ_n = Fixed χ offset used in modified-chi mode
 d = Interplanar spacing between crystallographic planes; also called d -spacing
 d_o = Interplanar spacing for unstressed material
 d_\perp = Perpendicular spacing
 Δd = Change in interplanar spacing caused by stress
 ε_{ij} = Strain component i, j
 E = Modulus of elasticity (Young's modulus)
 $E_{eff}^{(hkl)}$ = Effective elastic modulus for X-ray measurements
 μ = Attenuation coefficient
 η = Rotation of the sample around the measuring direction given by φ and ψ or χ and β
 ω or Ω = Angle between the specimen surface and incident beam when $\chi = 0^\circ$
 φ = Angle between the σ_{11} direction and measurement direction azimuth, see Fig. 1
 “ hkl ” = Miller indices
 σ_{ij} = Normal stress component i, j
 $s_1^{(hkl)}$ = X-ray elastic constant of quasi-isotropic material equal to $\frac{-\nu}{E_{eff}^{(hkl)}}$
 τ_{ij} = Shear stress component i, j
 θ = Bragg angle
 ν = Poisson's ratio
 x^{Mode} = Mode dependent depth of penetration
 ψ = Angle between the specimen surface normal and the scattering vector, that is, normal to the diffracting plane, see Fig. 1

4. Summary of Test Method

4.1 A test specimen is placed in a XRD goniometer aligned as per Test Method E915.

4.2 The diffraction profile is collected over three or more angles within the required angular range for a given $\{hkl\}$ plane, although at least seven or more are recommended.

4.3 The XRD profile data are then corrected for LPA, background, and instrument-specific corrections.

4.4 The peak position/Bragg angle is determined for each XRD peak profile.

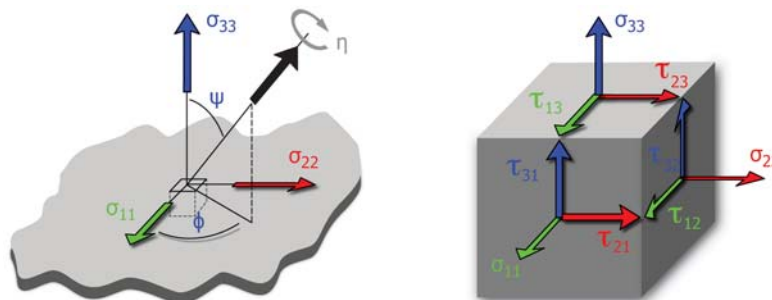


FIG. 1 Stress Tensor Components

4.5 The d -spacings are calculated from the peak positions via Bragg’s law.

4.6 The d -spacing values are plotted versus their $\sin^2\psi$ or $\sin^2\beta$ values, and the residual stress is calculated using Eq 4 or Eq 8, respectively.

4.7 The error in measurement is evaluated as per Section 14.

4.8 The following additional corrections may be applied. The use of these corrections shall be clearly indicated with the reported results.

4.8.1 Depth of penetration correction (see 12.12) and

4.8.2 Relaxation as a result of material removal correction (see 12.14).

5. Significance and Use

5.1 This test method covers a procedure for experimentally determining macroscopic residual stress tensor components of quasi-isotropic bearing steel materials by XRD. Here the stress components are represented by the tensor σ_{ij} as shown in Eq 1 (1,5 p. 40). The stress strain relationship in any direction of a component is defined by Eq 2 with respect to the azimuth phi(ϕ) and polar angle psi(ψ) defined in Fig. 1 (1, p. 132).

$$\sigma_{ij} = \begin{bmatrix} \sigma_{11} & \tau_{12} & \tau_{13} \\ \tau_{21} & \sigma_{22} & \tau_{23} \\ \tau_{31} & \tau_{32} & \sigma_{33} \end{bmatrix} \quad \text{where } \tau_{ij} = \tau_{ji} \quad (1)$$

⁵ The boldface numbers in parentheses refer to the list of references at the end of this standard.

$$\begin{aligned} \varepsilon_{\phi\psi}^{(hkl)} = & \frac{1}{2} s_2^{(hkl)} [\sigma_{11} \cos^2\phi \sin^2\psi + \sigma_{22} \sin^2\phi \sin^2\psi + \sigma_{33} \cos^2\psi] \\ & + \frac{1}{2} s_2^{(hkl)} [\tau_{12} \sin(2\phi) \sin^2\psi + \tau_{13} \cos\phi \sin(2\psi) + \tau_{23} \sin\phi \sin(2\psi)] \\ & + s_1^{(hkl)} [\sigma_{11} + \sigma_{22} + \sigma_{33}] \end{aligned} \quad (2)$$

5.1.1 Alternatively, Eq 2 may also be shown in the following arrangement (2, p. 126):

$$\begin{aligned} \varepsilon_{\phi\psi}^{(hkl)} = & \frac{1}{2} s_2^{(hkl)} [\sigma_{11} \cos^2\phi + \tau_{12} \sin(2\phi) + \sigma_{22} \sin^2\phi - \sigma_{33}] \sin^2\psi \\ & + \frac{1}{2} s_2^{(hkl)} \sigma_{33} - s_1^{(hkl)} [\sigma_{11} + \sigma_{22} + \sigma_{33}] + \frac{1}{2} s_2^{(hkl)} [\tau_{13} \cos\phi \\ & + \tau_{23} \sin\phi] \sin(2\psi) \end{aligned}$$

5.2 Using XRD and Bragg’s law, interplanar strain measurements are performed for multiple orientations. The orientations are selected based on a modified version of Eq 2, which is dictated by the mode used. Conflicting nomenclature may be found in literature with regard to mode names. For example, what may be referred to as a ψ (psi) diffractometer in Europe may be called a χ (chi) diffractometer in North America. The three modes considered here will be referred to as omega, chi, and modified-chi as described in 9.5.

5.3 Omega Mode (Iso Inclination) and Chi Mode (Side Inclination)—Interplanar strain measurements are performed at multiple ψ angles along one ϕ azimuth (let $\phi = 0^\circ$) (Figs. 2 and 3), reducing Eq 2 to Eq 3. Stress normal to the surface (σ_{33}) is assumed to be insignificant because of the shallow depth of penetration of X-rays at the free surface, reducing Eq 3 to Eq

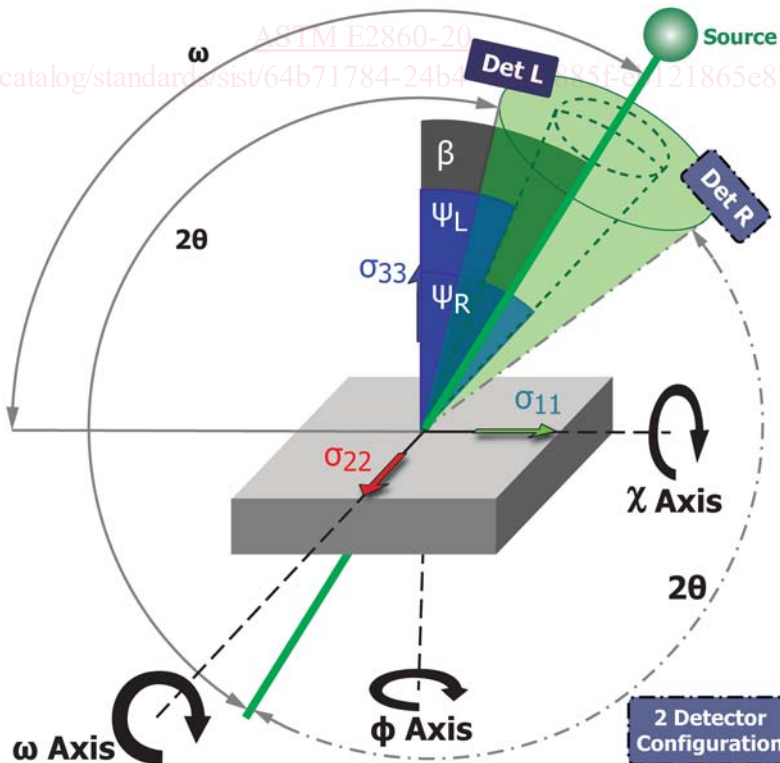
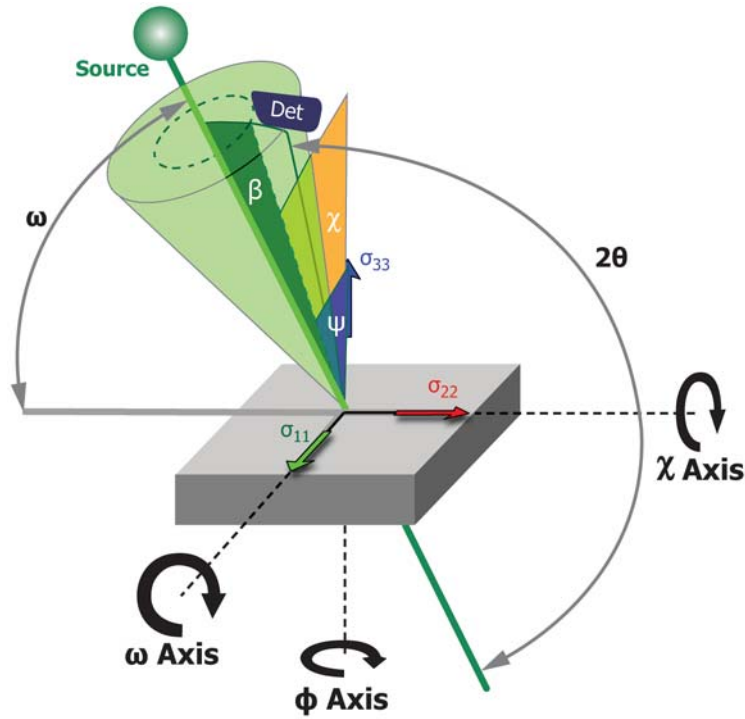


FIG. 2 Omega Mode Diagram for Measurement in σ_{11} Direction



NOTE 1—Stress matrix is rotated 90° about the surface normal compared to Fig. 2 and Fig. 14.
FIG. 3 Chi Mode Diagram for Measurement in σ_{11} Direction

4. Post-measurement corrections may be applied to account for possible σ_{33} influences (12.12). Since the σ_{ij} values will remain constant for a given azimuth, the $s_1^{\{hkl\}}$ term is renamed C .

$$\varepsilon_{\phi\psi}^{\{hkl\}} = \frac{1}{2}s_2^{\{hkl\}} [\sigma_{11} \sin^2\psi + \sigma_{33} \cos^2\psi] + \frac{1}{2}s_2^{\{hkl\}} [\tau_{13}\sin(2\psi)] + s_1^{\{hkl\}} [\sigma_{11} + \sigma_{22} + \sigma_{33}] \quad (3)$$

$$\varepsilon_{\phi\psi}^{\{hkl\}} = \frac{1}{2}s_2^{\{hkl\}} [\sigma_{11} \sin^2\psi + \tau_{13}\sin(2\psi)] + C \quad (4)$$

5.3.1 The measured interplanar spacing values are converted to strain using Eq 24, Eq 25, or Eq 26. Eq 4 is used to fit the strain versus $\sin^2\psi$ data yielding the values σ_{11} , τ_{13} , and C . The measurement can then be repeated for multiple phi angles (for example 0, 45, and 90°) to determine the full stress/strain tensor. The value, σ_{11} , will influence the overall

slope of the data, while τ_{13} is related to the direction and degree of elliptical opening. Fig. 4 shows a simulated d versus $\sin^2\psi$ profile for the tensor shown. Here the positive 20-MPa τ_{13} stress results in an elliptical opening in which the positive psi range opens upward and the negative psi range opens downward. A higher τ_{13} value will cause a larger elliptical opening. A negative 20-MPa τ_{13} stress would result in the same elliptical opening only the direction would be reversed with the positive psi range opening downwards and the negative psi range opening upwards as shown in Fig. 5.

5.4 Modified Chi Mode—Interplanar strain measurements are performed at multiple β angles with a fixed χ offset, χ_m (Fig. 6). Measurements at various β angles do not provide a constant ϕ angle (Fig. 7), therefore, Eq 2 cannot be simplified in the same manner as for omega and chi mode.

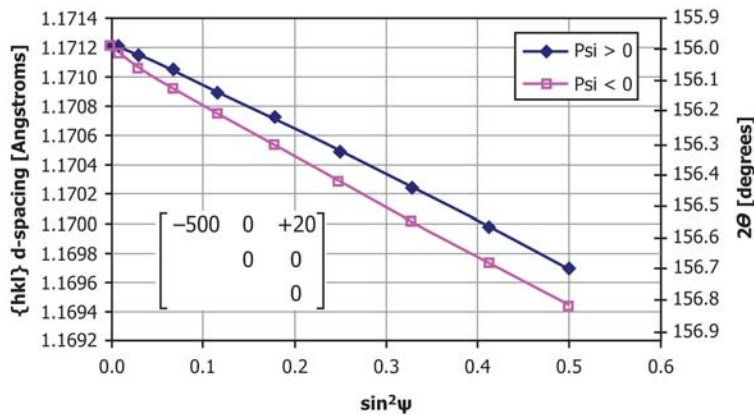


FIG. 4 Sample $d(2\theta)$ Versus $\sin^2\psi$ Dataset with $\sigma_{11} = -500$ MPa and $\tau_{13} = +20$ MPa

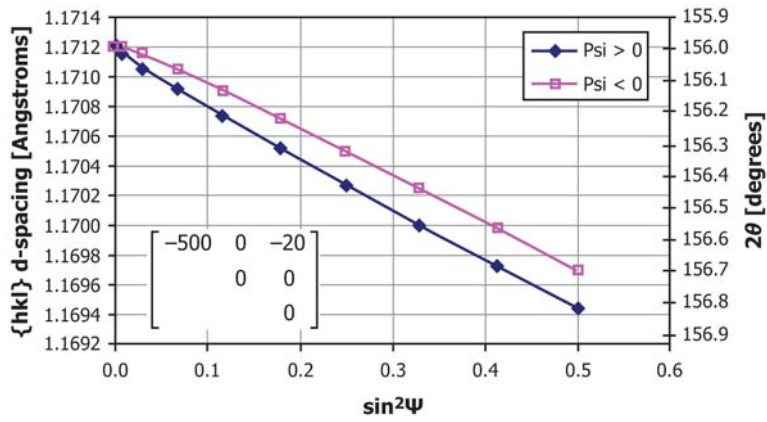


FIG. 5 Sample $d(2\theta)$ Versus $\sin^2\Psi$ Dataset with $\sigma_{11} = -500$ MPa and $\tau_{13} = -20$ MPa

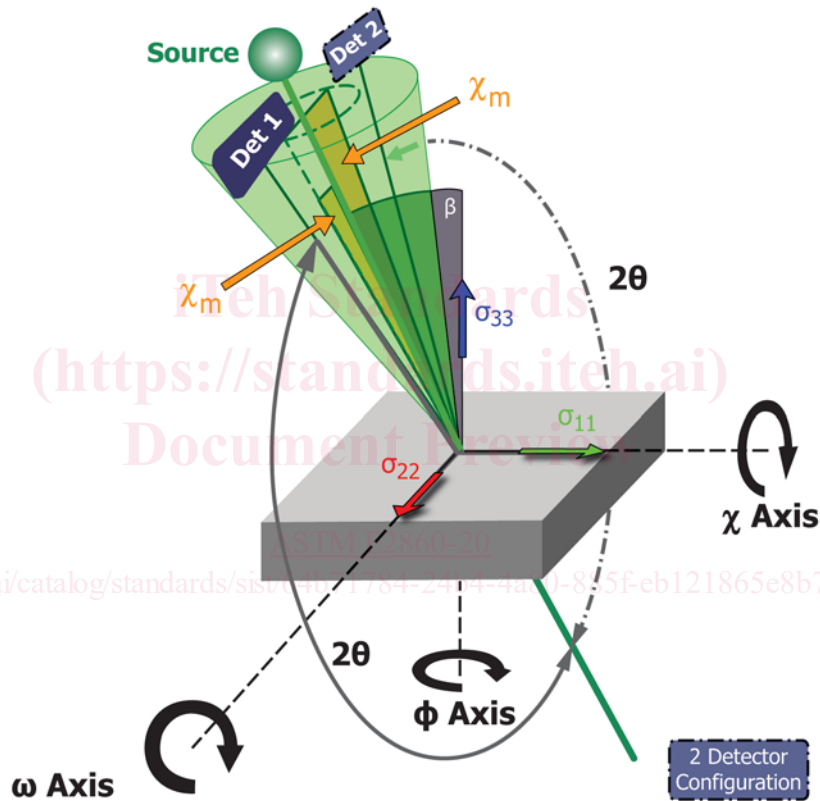


FIG. 6 Modified Chi Mode Diagram for Measurement in σ_{11} Direction

5.4.1 Eq 2 shall be rewritten in terms of β and χ_m . Eq 5 and 6 are obtained from the solution for a right-angled spherical triangle (3).

$$\psi = \arccos(\cos \beta \cos \chi_m) \quad (5)$$

$$\phi = \arccos\left(\frac{\sin \beta \cos \chi_m}{\sin \psi}\right) \quad (6)$$

5.4.2 Substituting ϕ and ψ in Eq 2 with Eq 5 and 6 (see X1.1), we get:

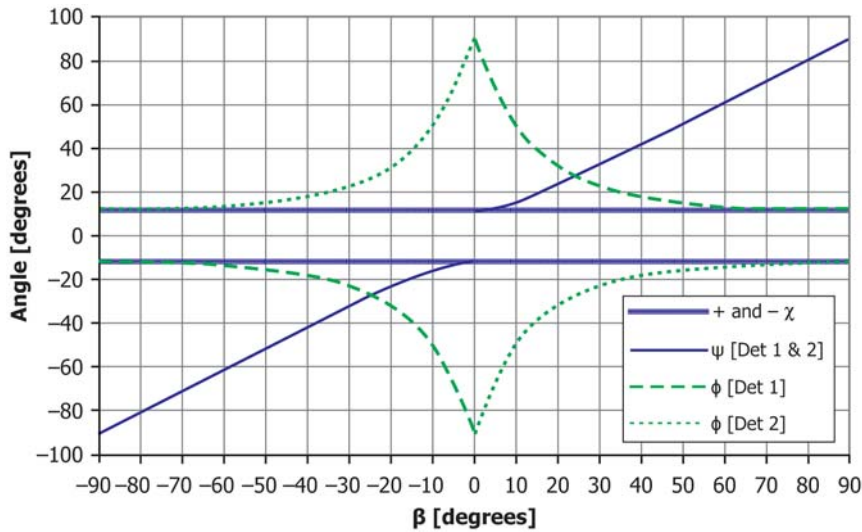


FIG. 7 ψ and ϕ Angles Versus β Angle for Modified Chi Mode with $\chi_m = 12^\circ$

$$\begin{aligned} \varepsilon_{\beta\chi_m}^{\{hkl\}} &= \frac{1}{2}s_2^{\{hkl\}} [\sigma_{11} \sin^2\beta \cos^2\chi_m + \sigma_{22} \sin^2\chi_m + \sigma_{33} \cos^2\beta \cos^2\chi_m] \\ &+ \frac{1}{2}s_2^{\{hkl\}} [\tau_{12}\sin\beta\sin(2\chi_m) + \tau_{13}\sin(2\beta) \cos^2\chi_m + \tau_{23}\cos\beta\sin(2\chi_m)] \\ &+ s_1^{\{hkl\}} [\sigma_{11} + \sigma_{22} + \sigma_{33}] \end{aligned} \quad (7)$$

5.4.3 Stress normal to the surface (σ_{33}) is assumed to be insignificant because of the shallow depth of penetration of X-rays at the free surface reducing Eq 7 to Eq 8. Post-measurement corrections may be applied to account for possible σ_{33} influences (see 12.12). Since the σ_{ij} values and χ_m will remain constant for a given azimuth, the $s_1^{\{hkl\}}$ term is renamed C , and the σ_{22} term is renamed D .

$$\begin{aligned} \varepsilon_{\beta\chi_m}^{\{hkl\}} &= \frac{1}{2}s_2^{\{hkl\}} [\sigma_{11} \sin^2\beta \cos^2\chi_m + D] + \frac{1}{2}s_2^{\{hkl\}} [\tau_{12}\sin\beta\sin(2\chi_m) \\ &+ \tau_{13}\sin(2\beta) \cos^2\chi_m + \tau_{23}\cos\beta\sin(2\chi_m)] + C \end{aligned} \quad (8)$$

5.4.4 The σ_{11} influence on the d versus $\sin^2\beta$ plot is similar to omega and chi mode (Fig. 8) with the exception that the slope shall be divided by $\cos^2\chi_m$. This increases the effective $1/2 s_2^{\{hkl\}}$ by a factor of $1/\cos^2\chi_m$ for σ_{11} .

5.4.5 The τ_{ij} influences on the d versus $\sin^2\beta$ plot are more complex and are often assumed to be zero (3). However, this may not be true and significant errors in the calculated stress may result. Figs. 9-13 show the d versus $\sin^2\beta$ influences of individual shear components for modified chi mode considering two detector positions ($\chi_m = +12^\circ$ and $\chi_m = -12^\circ$). Components τ_{12} and τ_{13} cause a symmetrical opening about the σ_{11} slope influence for either detector position (Figs. 9-11); therefore, σ_{11} can still be determined by simply averaging the positive and negative β data. Fitting the opening to the τ_{12} and τ_{13} terms may be possible, although distinguishing between the two influences through regression is not normally possible.

5.4.6 The τ_{23} value affects the d versus $\sin^2\beta$ slope in a similar fashion to σ_{11} for each detector position (Figs. 12 and 13). This is an unwanted effect since the σ_{11} and τ_{23} influence cannot be resolved for one χ_m position. In this instance, the τ_{23} shear stress of -100 MPa results in a calculated σ_{11} value of -472.5 MPa for $\chi_m = +12^\circ$ or -527.5 MPa for $\chi_m = -12^\circ$, while the actual value is -500 MPa. The value, σ_{11} can still be determined by averaging the β data for both χ_m positions.

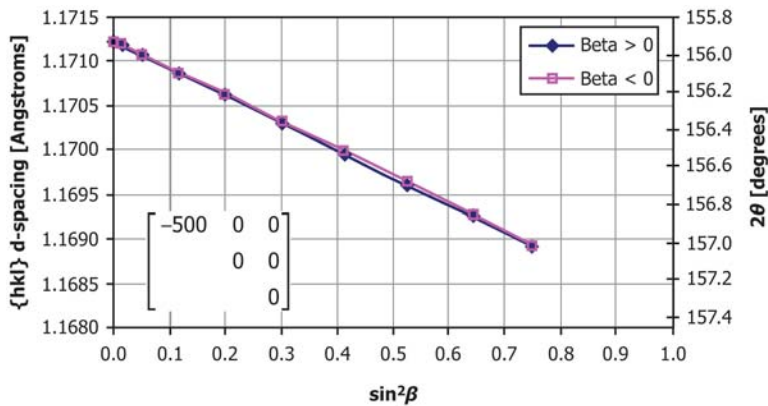


FIG. 8 Sample $d(2\theta)$ Versus $\sin^2\beta$ Dataset with $\sigma_{11} = -500$ MPa

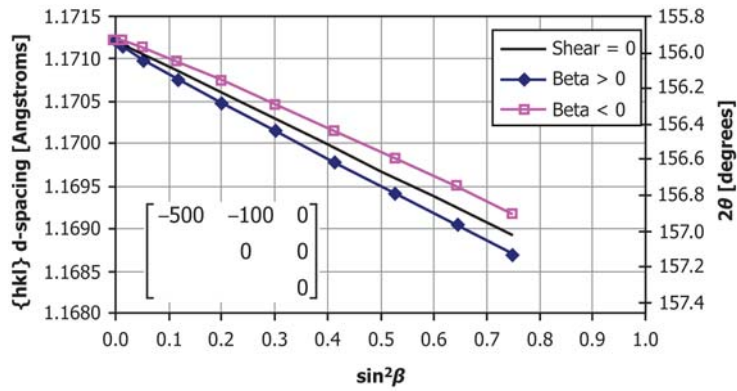


FIG. 9 Sample $d(2\theta)$ versus $\sin^2\beta$ Dataset with $\chi_m = +12^\circ$, $\sigma_{11} = -500$ MPa, and $\tau_{12} = -100$ MPa

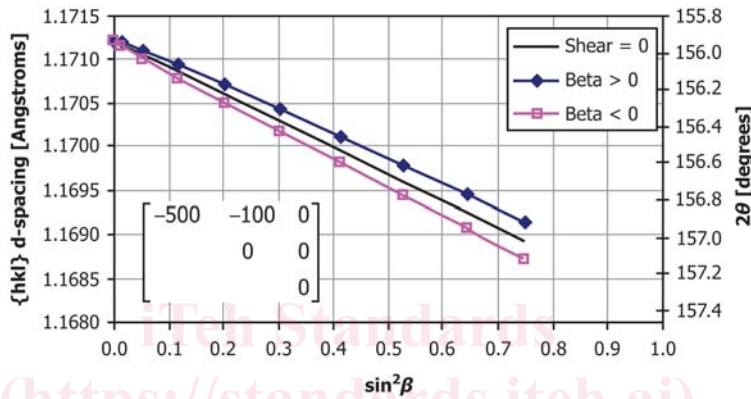


FIG. 10 Sample $d(2\theta)$ Versus $\sin^2\beta$ Dataset with $\chi_m = -12^\circ$, $\sigma_{11} = -500$ MPa, and $\tau_{12} = -100$ MPa

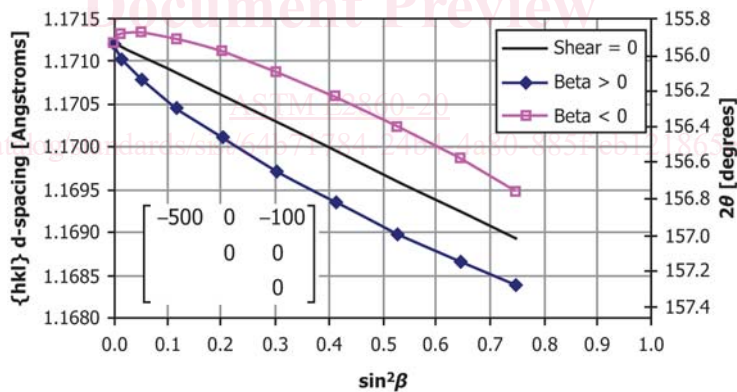


FIG. 11 Sample $d(2\theta)$ Versus $\sin^2\beta$ Dataset with $\chi_m = +12$ or -12° , $\sigma_{11} = -500$ MPa, and $\tau_{13} = -100$ MPa

5.4.7 The use of the modified chi mode may be used to determine σ_{11} but shall be approached with caution using one χ_m position because of the possible presence of a τ_{23} stress. The combination of multiple stresses including τ_{23} results in increasingly complex shear influences. Chi and omega mode are preferred over modified chi for these reasons.

6. Apparatus

6.1 A typical X-ray diffractometer is composed of the following main components:

6.1.1 *Goniometer*—An angle-measuring device responsible for the positioning of the source, detectors, and sample relative to each other.

6.1.2 *X-Ray Source*—There are generally three X-ray sources used for XRD.

6.1.2.1 *Conventional Sealed Tube*—This is by far the most common found in XRD equipment. It is identified by its anode target element such as chromium (Cr), manganese (Mn), or copper (Cu). The anode is bombarded by electrons to produce specific X-ray wavelengths unique to the target element.

6.1.2.2 *Rotating Anode Tube*—This style of tube offers a higher intensity than a conventional sealed tube.

6.1.2.3 *Synchrotron*—Particle accelerator that is capable of producing a high-intensity X-ray beam.

6.1.2.4 *Sealed Radioactive Sources*—Although not commonly used, they may be utilized.